Applied Physics Letters ARTICLE pubs.aip.org/aip/apl

First-principles prediction of thermal conductivity of bulk hexagonal boron nitride

Cite as: Appl. Phys. Lett. **124**, 163906 (2024); doi: 10.1063/5.0210935
Submitted: 27 March 2024 · Accepted: 2 April 2024 ·
Published Online: 17 April 2024

Ziqi Guo, Zherui Han, Abdulaziz Alkandari, Krutarth Khot, and Xiulin Ruan[a)]

AFFILIATIONS

Department of Mechanical Engineering and the Birck Nanotechnology Center, Purdue University, West Lafayette, Indiana 47907, USA

Note: This paper is part of the APL Special Collection on Advances in Thermal Phonon Engineering and Thermal Management.
[a)]**Author to whom correspondence should be addressed:** ruan@purdue.edu

ABSTRACT

Despite its importance, a sophisticated theoretical study of thermal conductivity in bulk h-BN has been lacking to date. In this study, we predict thermal conductivity in bulk h-BN crystals using first-principles predictions and the Boltzmann transport equation. We consider three-phonon (3ph) scattering, four-phonon (4ph) scattering, and phonon renormalization. Our predicted thermal conductivity is 363 and 4.88 W/(m K) for the in-plane and out-of-plane directions at room temperature, respectively. Further analysis reveals that 4ph scattering reduces thermal conductivity, while phonon renormalization weakens phonon anharmonicity and increases thermal conductivity. Eventually, the in-plane and out-of-plane thermal conductivities show intriguing $\sim T^{-0.627}$ and $\sim T^{-0.568}$ dependencies, respectively, far deviating from the traditional 1/T relation.

In recent years, two-dimensional (2D) materials have drawn great interest in the scientific community due to their unique properties and promising applications in nanoelectronics. Many interesting 2D material systems with exceptional electrical, thermal, and mechanical properties are investigated.[1–6] Among these, hexagonal boron nitride (h-BN) is of particular interest due to its intriguing properties, including wide electronic bandgap, high thermal stability, and highly anisotropic thermal and optical properties. h-BN has been widely used in transistors,[7–9] phonon-polariton nanophotonic devices,[10,11] ultraviolet light emitters,[12] single-photon sources,[13] lubrication,[14] radiative cooling,[15] etc.

The thermal conductivity (κ) is critical in many applications of h-BN. Originating from the strong intralayer covalent bonds and weak interlayer van der Waal bonds, the thermal conductivity of h-BN is highly anisotropic, which is favored in many applications including the substrate for electronic devices[16] and thermal interfacial materials.[17–20] Therefore, it is important to develop a detailed understanding of thermal transport properties in h-BN.

First-principles calculation based on density functional theory (DFT) and Boltzmann transport equation (BTE) has been proven to accurately predict thermal conductivity. The inception of the phonon BTE can be traced back to the foundational work by Peierls,[21] which was subsequently extended through the development of three-phonon (3ph) scattering theory by Maradudin and Fein.[22] Building upon this foundation, first-principles calculations were used to predict 3ph scattering rates for the zone-center optical phonon linewidth;[23,24] Broido *et al.* integrated these approaches with *ab initio* force constants to facilitate the first-principles prediction of thermal conductivity, thereby significantly advancing the understanding of thermal transport mechanisms.[25–28] Recently, Feng and Ruan developed the general theory and computational method for four-phonon (4ph) scattering and predicted its importance in a range of materials and temperatures.[29,30] The prediction on boron arsenide was subsequently confirmed by independent experiments,[31–33] and it has been demonstrated that considering 4ph scattering would considerably reduce the thermal conductivity in various materials.[34–37] Furthermore, the force constants can deviate from that given by the traditional perturbative approach at 0 K due to the finite temperature effect that leads to the phonon renormalization.[38] It was shown that both 4ph scattering and phonon renormalization are important components in the accurate prediction of thermal conductivity as temperature rises.[39–43]

A few first-principles calculations have been performed on bulk hBN. Jiang *et al.*[44] considered 3ph scattering, and the thermal conductivity for the in-plane direction was overpredicted. Tang *et al.*[45] considered both the 3ph and 4ph scattering effects, while the 4ph scattering rates are calculated with machine learning potentials to reduce the computational cost. Their predicted result is lower than the experimental value. Notably, the phonon renormalization effect has not been

considered in these studies. It is imperative to gain a comprehensive understanding of thermal transport phenomena in bulk h-BN that considers all phonon interactions.

In this Letter, we study the thermal transport properties of bulk h-BN based on the first-principles prediction over the temperature range of 200–700 K. Our calculated result agrees well with the measured data reported in the literature. We then analyze the effect of 4ph scattering and phonon renormalization on phonon transport. The thermal conductivity is greatly reduced by 4ph scattering, while the phonon renormalization weakens both 3ph and 4ph scattering strength and subsequently increases the predicted thermal conductivity. In addition, despite the commonly established 1/T temperature dependence of thermal conductivity for many materials, we found that h-BN exhibits a weaker temperature dependence, which is attributed to the contribution of high-frequency phonon modes. We also investigate the size effect of phonon transport.

We performed DFT calculations using the Vienna *Ab initio* Simulation Package (VASP).[46] For the exchange-correlation function, we employed the local density approximation (LDA)[47] with the projector augmented wave (PAW) method.[48] LDA has also been used in previous studies investigating h-BN's properties including phonon dispersion,[49,50] thermal conductivity,[44,45,51] and Raman linewidth.[52] The lattice constant is relaxed with the electron energy convergence threshold of 10^{-8} eV and the force convergence threshold of 10^{-7} eV/Å.

Following structural optimization, we calculated the harmonic and anharmonic interatomic force constants (IFCs) with the perturbative approach at 0 K. The DFT calculations of all the IFCs were performed with a cutoff energy of 700 eV, utilizing a $5 \times 5 \times 2$ supercell and a $3 \times 3 \times 3$ k-mesh for sampling the Brillouin zone. For the harmonic calculations, we employed density functional perturbation theory (DFPT)[53] using PHONOPY.[54] Non-analytical term correction was applied to include the long-range dipole–dipole interaction, with the Born effective charge tensor and high-frequency dielectric tensor determined from DFPT. The anharmonic IFCs were calculated using the finite displacement method with cutoff radii of 4.3 and 3.7 Å for third-order and fourth-order IFCs calculations, respectively. The displacement value is chosen as 0.01 Å. As Zhou *et al.*[55] demonstrate that the higher-order force constant is sensitive to displacement, we also studied the influence of the displacement parameter on thermal conductivity and found the impact on hBN to be small, which is shown in Fig. S1.

We then considered the effect of phonon renormalization. We acquired the lattice thermal expansion coefficients from simulation conducted by Niu *et al.*,[56] which is based on quasi-harmonic approximation and has a good agreement with the experimental results.[57] To calculate the effective IFCs that can best describe the interatomic potential, we employed a temperature-dependent effective potential (TDEP) method.[58] The effective IFCs were obtained through an iterative process that begins with collecting datasets of force-displacement pairs and subsequently minimizing the force differences to refine the IFCs. The effective harmonic IFC can be obtained through the following minimization procedure:

$$\min_{\Phi_2^*} \Delta \mathbf{F} = \frac{1}{N_t} \sum_{t=1}^{N_t} \left(\mathbf{F}_t - \mathbf{F}_t^{\mathrm{H}} \right)^2, \tag{1}$$

where Φ_2^* is the effective harmonic IFC, N_t is the size of the force-displacement dataset, $\mathbf{F_t}$ is the force calculated through DFT with certain displacement, and $\mathbf{F}_t^{\mathrm{H}}$ is the force calculated using the effective IFCs. The anharmonic IFCs can be obtained from a similar minimization process. After reaching convergence, we obtained a set of effective IFCs that can accurately describe the potential landscape at finite temperatures. A detailed description of this method can be found in Refs. 38, 58, and 59. In this work, we conducted six iterations using 100 thermally perturbed snapshots generated from Bose–Einstein distributions at each iteration to ensure convergence of phonon dispersion and thermal conductivity.

The thermal conductivity is predicted using the ShengBTE package integrated with FourPhonon module,[60,61] with a $22 \times 22 \times 12$ **q**-mesh size. In this study, 3ph scattering was iteratively solved, while 4 ph scattering was solved under single mode relaxation time approximation (SMRTA). Calculating phonon scattering is known to be highly computationally expensive, and several works have been done to mitigate the computational cost, such as utilizing GPU parallel computing ability[62,63] and machine learning.[64] Here, we adopted a sampling-estimation approach where the 4ph scattering rates were estimated from a subset of all phonon scattering events.[65] The sample size is chosen to be 10^6.

Figure 1(a) shows the lattice structure of h-BN for our study. Given that bulk h-BN is a layered material with various stacking possibilities, we specifically adopted the AA′ stacking order, which has been confirmed through atomic resolution imaging and is known for its stability.[66–68] A full structural optimization gives the lattice constants of $a = 2.490$ and $c = 6.476$ Å. Figure 1(b) shows the phonon dispersion calculated with and without phonon renormalization at 300 K. The calculated phonon dispersion has a good agreement with the experimental measurement.[49] We also provide the phonon dispersion at 600 K in Fig. S2.

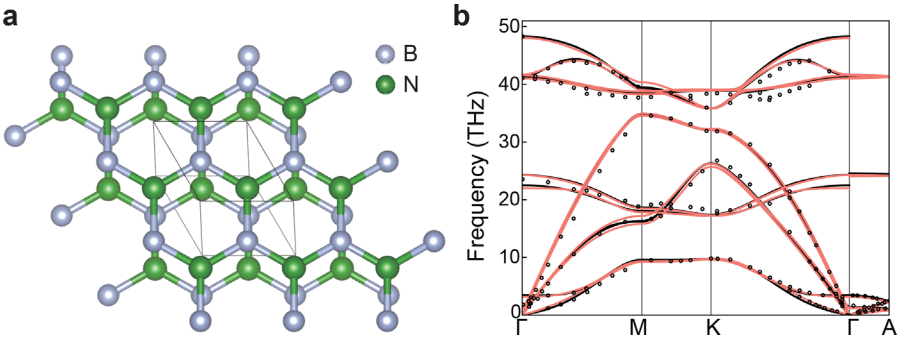

FIG. 1. Lattice structure and phonon dispersion of bulk h-BN. (a) Lattice structure of h-BN from a perspective view. The black wireframe shows one unit cell. (b) The phonon dispersion of bulk h-BN calculated with (red lines) and without (black lines) phonon renormalization at 300 K compared with the experiment[49] (black dots).

The thermal conductivity from 200 to 700 K is then predicted, as shown in Fig. 2. The green dashed line shows the result with only 3ph scattering. The inclusion of 4ph scattering (red dash line) leads to a notable reduction in thermal conductivity, in both the in-plane and out-of-plane directions. Subsequently, when we consider the phonon renormalization (red solid line), our predicted thermal conductivity increases and agrees, coincidentally, with the results obtained solely from 3ph scattering at 0 K for in-plane direction. For the out-of-plane direction, the predicted thermal conductivity becomes slightly higher than that from 3ph scattering at 0 K. The temperature dependency of thermal conductivity is strengthened after including 4ph scattering, from $\sim T^{-0.650}$ and $\sim T^{-0.524}$ to $\sim T^{-0.652}$ and $\sim T^{-0.789}$ for in-plane and out-of-plane direction, respectively. After including the phonon renormalization effect, the temperature dependency becomes weaker and goes to $\sim T^{-0.627}$ and $\sim T^{-0.568}$, respectively. We found that the temperature dependency is much weaker than the well-known 1/T relation, which will be discussed later. We also calculated the contribution of the diffuson-like phonons and found their contributions quite small in general. Due to the much lower thermal conductivity in the cross-plane direction than in the in-plane direction, the contribution of diffuson-like phonons is relatively more important for the cross-plane direction. Details can be found in Fig. S3 of the supplementary material.

We compare our predicted result to experimental data from the literature. After incorporating both 4ph scattering and phonon renormalization into our calculations, our predicted in-plane thermal conductivity demonstrates excellent agreement with the experimental result reported by Sichel *et al.*[69] Our result is slightly lower than those reported by Jiang *et al.*[44] and Yuan *et al.*[51] but close to the experimental error bars. In the out-of-plane direction, our result agrees well with the experiments. It is worth noting that Salihoglu *et al.*[70] considered the radiation heat transfer between different layers of bulk h-BN in their out-of-plane thermal conductivity measurements, which is non-negligible due to its hyperbolic dispersion characteristic. After eliminating the contribution of radiation heat transfer from the total thermal conductivity, our results closely match the thermal conductivity attributed to phonon transport. Moreover, although the experimental thermal conductivity has an apparent agreement with the predicted result considering solely 3ph scattering at 0 K, the agreement is coincidental. This agreement primarily arises from the omission of both 4ph scattering and phonon renormalization, leading to an error-canceling effect that conceals important physical details.

Compared with other simulation results, Jiang *et al.*[44] include only the 3ph scattering effect. The predicted values match with our 3ph results for the out-of-plane direction. However, in the case of the in-plane direction, their predictions exceed our results, potentially attributable to a small in-plane cutoff radius when calculating IFCs. Tang *et al.*[45] include both 3ph and 4ph scattering. The results show a slight deviation from our 3ph + 4ph results, which could be attributed to the small **q**-mesh in solving BTE as well as the use of machine learning potentials to assess the 4ph scattering rates.

To gain a deeper understanding of the phonon scattering in h-BN, Fig. 3(a) shows 3ph and 4ph scattering rates and how they are affected by phonon renormalization. Both 3ph and 4ph scattering are weakened after including the phonon renormalization, which is the reason for the higher thermal conductivity prediction. Moreover, there is a more substantial reduction in 4ph scattering rates, indicating that the higher-order anharmonicity is affected more at finite temperatures. Figure 3(b) shows the phonon scattering rates across a temperature range spanning from 200 to 700 K, where 3ph and 4ph scattering and phonon renormalization are included. As temperature increases, phonon scattering becomes stronger, primarily due to an increase in phonon population, which obeys the Bose–Einstein distribution: $n_\lambda^0 = 1/(e^{\hbar\omega_\lambda/k_B T} - 1)$. The rise in phonon scattering rates leads to the reduction in thermal conductivity.

We now discuss the deviation of the temperature dependence of both in-plane and out-of-plane thermal conductivity from the traditional $\kappa \sim 1/T$ law. This unusual dependency could be attributed to the contribution of high-frequency phonons. Figure 4 illustrates the thermal conductivity contributions from phonon modes with frequencies higher than 15 THz and separately from the other low-frequency phonon modes. 15 THz is chosen as the cutoff frequency since it separates the acoustic and breathing phonon modes and the optical phonon modes, particularly near the Γ point where acoustic and breathing phonon modes have large group velocities. Additionally, the frequency-accumulated thermal conductivity (Fig. S4) revealed that 15 THz serves as a dividing frequency for the contributions to the total thermal conductivity. For both in-plane and out-of-plane thermal conductivities, the low-frequency contributions follow the well-known 1/T relation. However, as the temperature increases, the contributions from high-frequency phonon modes increase, which suppress the 1/T relationship in the total thermal conductivity. The different temperature dependence of thermal conductivity for different frequencies is due to the competing effect of specific heat and phonon scattering.

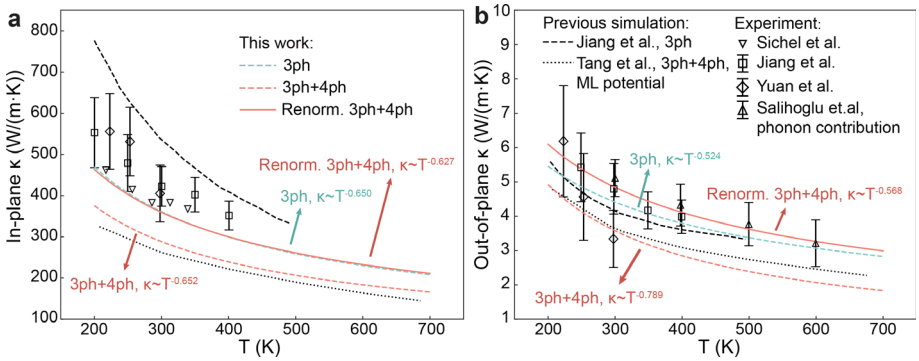

FIG. 2. Lattice thermal conductivity as a function of temperature for h-BN. (a) In-plane direction. (b) Out-of-plane direction. The results are compared with the measurement by Sichel *et al.*[69] (in-plane only), Jiang *et al.*,[44] Yuan *et al.*,[51] and Salihoglu *et al.*[70] (out-of-plane only, excluding radiation heat transfer) and the simulations by Jiang *et al.*[44] (3ph scattering only) and Tang *et al.*[45] (3ph and 4ph scattering calculated using machine learning potentials).

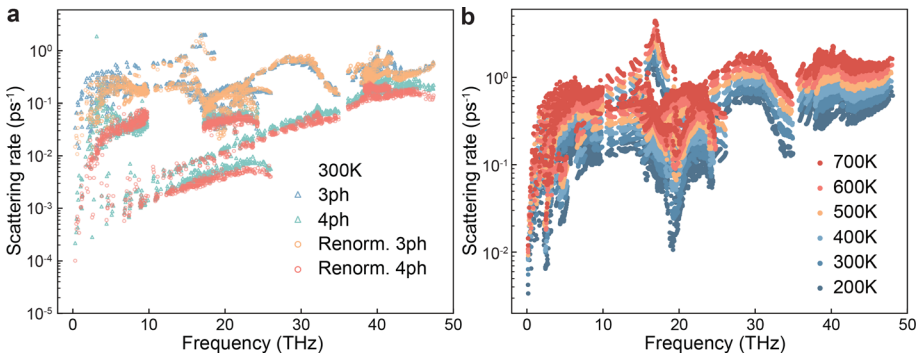

FIG. 3. Phonon scattering rate as a function of phonon frequency. (a) The 3ph and 4ph scattering rates at 300 K. Circle and triangle dots represent the scattering rates calculated with and without phonon renormalization at 300 K, respectively. (b) Temperature evolution of phonon scattering rates considering 3ph scattering, 4ph scattering, and phonon renormalization.

The specific heat can be qualitatively estimated based on the Einstein model,

$$C(T) = k_B \left(\frac{T_E}{T}\right)^2 \frac{e^{T_E/T}}{\left(e^{T_E/T}-1\right)^2}, \tag{2}$$

where T_E is the Einstein temperature ($T_E \equiv \hbar\omega_\lambda / k_B$), which is a characteristic temperature below which the thermal energy is insufficient to excite the phonon mode beyond their ground state. Since the high-frequency phonon modes have higher Einstein temperatures, they are "frozen out" at low temperatures and gradually excited as temperature increases. Consequently, their heat capacity exhibits a significant increase with rising temperature (see Fig. S5). This phenomenon leads to an initial increase in thermal conductivity at low temperatures due to the rapid rise in heat capacity. However, at higher temperatures, as the specific heat exhibits slower growth with temperature, the thermal conductivity decreases due to the increased prevalence of phonon scattering. In contrast, the low-frequency phonon modes are much easier to excite due to a low Einstein temperature and their specific heat already saturated at a low temperature. The temperature dependence of thermal conductivity is dominated by the phonon scattering part and shows a monotonically decreasing trend. This anomalous temperature dependence of thermal conductivity has also been observed in other 2D materials, including GaN,[71] h-AlN,[72] ZnO,[73] etc. However, most of these studies focus on monolayer materials, where only the in-plane thermal conductivity is considered. As for the previous study of h-BN, Jiang *et al.*[44] observed the anonymous temperature dependence only in the out-of-plane thermal conductivity, while the in-plane thermal conductivity follows the 1/T dependence in their simulation results. The discrepancy with our result could again be attributed to the small in-plane cutoff radius in their calculations. It is now shown that in a bulk 2D material like h-BN, such weakened temperature dependence of thermal conductivity exists in both in-plane and out-of-plane directions.

When designing nanostructures or nanodevices based on h-BN, effectively managing heat dissipation becomes crucial for ensuring their reliable operation. One key parameter that provides valuable insights into the size-dependent thermal conductivity is the phonon mean free path (MFP). Figure 5 shows the accumulated thermal conductivity with respect to MFP for both in-plane and out-of-plane directions at various temperatures. The representative MFP, defined as the MFP corresponding to 50% cumulative thermal conductivity, decreases as the temperature increases. In addition, at 300 K, phonons with MFPs under 586 and 278 nm contribute to 90% of the in-plane and out-of-plane thermal conductivity, respectively. This shows that for designing h-BN-based devices with characteristic lengths less than around 600 nm, the size effect should be considered.

To summarize, we present a comprehensive study of the thermal transport in bulk h-BN through first-principles calculation spanning temperatures from 200 to 700 K. We include the mechanism of three-phonon scattering, four-phonon scattering, as well as phonon renormalization. Our predicted thermal conductivity exhibits good agreement with the experimental result in the literature. We also investigate the scattering rates, the anomalous temperature dependence of thermal conductivity, and the size-dependent thermal conductivity. This work provides fundamental insights into the microscopic mechanisms governing phonon transport in h-BN and contributes to a deeper understanding of thermal transport in highly anisotropic layered crystals.

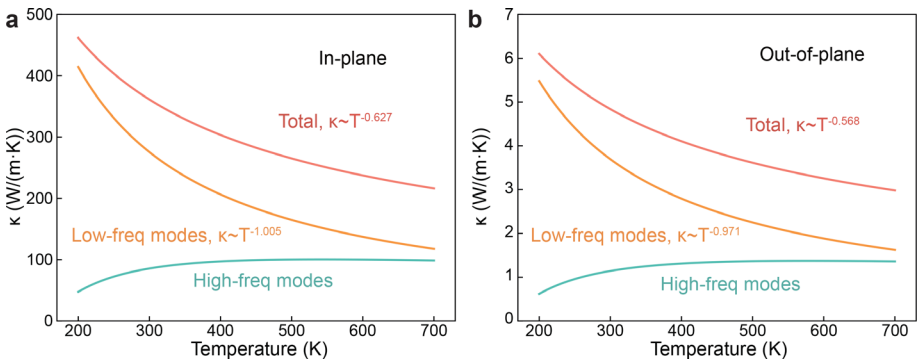

FIG. 4. Thermal conductivity contribution from high- and low-frequency phonon modes. (a) In-plane direction. (b) Out-of-plane direction.

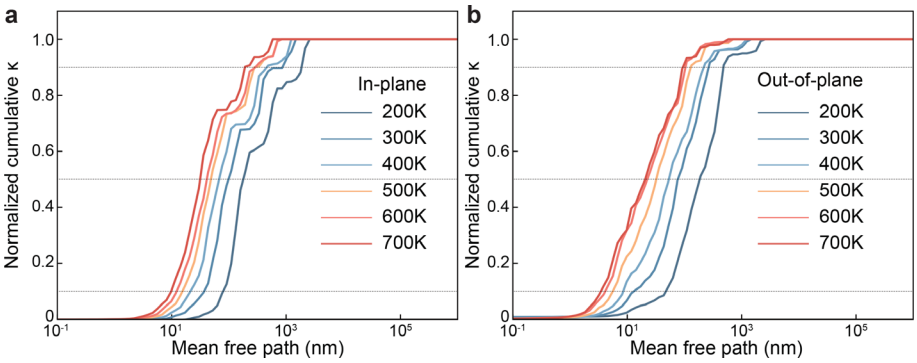

FIG. 5. Normalized cumulative thermal conductivity of h-BN as a function of phonon mean free path from 200 to 700 K. (a) In-plane direction. (b) Out-of-plane direction. The three dash lines stand for 10%, 50%, and 90% of total thermal conductivity, respectively.

See the supplementary material for detailed information on the impact of displacement parameter and diffuson-like phonon, phonon dispersion, cumulative thermal conductivity, and temperature and frequency dependency of heat capacity.

Z.G., Z.H., K.K., and X.R. acknowledge partial support from NSF Award Nos. 2311848 and 2321301. Simulations were performed at the Rosen Center for Advanced Computing (RCAC) of Purdue University.

AUTHOR DECLARATIONS

Conflict of Interest

The authors have no conflicts to disclose.

Author Contributions

Ziqi Guo: Conceptualization (lead); Data curation (lead); Formal analysis (lead); Investigation (lead); Methodology (lead); Validation (lead); Visualization (lead); Writing – original draft (lead); Writing – review & editing (lead). **Zherui Han:** Data curation (supporting); Methodology (supporting); Writing – review & editing (supporting). **Abdulaziz Alkandari:** Data curation (supporting); Methodology (supporting); Writing – review & editing (supporting). **Krutarth Khot:** Data curation (supporting); Methodology (supporting); Writing – review & editing (supporting). **Xiulin Ruan:** Funding acquisition (lead); Project administration (lead); Resources (lead); Supervision (lead); Writing – review & editing (supporting).

DATA AVAILABILITY

The data that support the findings of this study are available from the corresponding author upon reasonable request.

REFERENCES

[1]K. S. Novoselov, A. K. Geim, S. V. Morozov, D-e Jiang, Y. Zhang, S. V. Dubonos, I. V. Grigorieva, and A. A. Firsov, "Electric field effect in atomically thin carbon films," Science **306**, 666–669 (2004).
[2]A. A. Balandin, "Thermal properties of graphene and nanostructured carbon materials," Nat. Mater. **10**, 569–581 (2011).
[3]D. G. Papageorgiou, I. A. Kinloch, and R. J. Young, "Mechanical properties of graphene and graphene-based nanocomposites," Prog. Mater. Sci. **90**, 75–127 (2017).
[4]M. Turunen, M. Brotons-Gisbert, Y. Dai, Y. Wang, E. Scerri, C. Bonato, K. D. Jöns, Z. Sun, and B. D. Gerardot, "Quantum photonics with layered 2D materials," Nat. Rev. Phys. **4**, 219–236 (2022).
[5]M. C. Lemme, D. Akinwande, C. Huyghebaert, and C. Stampfer, "2D materials for future heterogeneous electronics," Nat. Commun. **13**, 1392 (2022).
[6]G. Fiori, F. Bonaccorso, G. Iannaccone, T. Palacios, D. Neumaier, A. Seabaugh, S. K. Banerjee, and L. Colombo, "Electronics based on two-dimensional materials," Nat. Nanotechnol. **9**, 768–779 (2014).
[7]C. R. Dean, A. F. Young, I. Meric, C. Lee, L. Wang, S. Sorgenfrei, K. Watanabe, T. Taniguchi, P. Kim, K. L. Shepard *et al.*, "Boron nitride substrates for high-quality graphene electronics," Nat. Nanotechnol. **5**, 722–726 (2010).
[8]L. Ponomarenko, A. Geim, A. Zhukov, R. Jalil, S. Morozov, K. Novoselov, I. Grigorieva, E. Hill, V. Cheianov, V. Fal'Ko *et al.*, "Tunable metal–insulator transition in double-layer graphene heterostructures," Nat. Phys. **7**, 958–961 (2011).
[9]L. Britnell, R. Gorbachev, R. Jalil, B. Belle, F. Schedin, A. Mishchenko, T. Georgiou, M. Katsnelson, L. Eaves, S. Morozov *et al.*, "Field-effect tunneling transistor based on vertical graphene heterostructures," Science **335**, 947–950 (2012).
[10]P. Li, M. Lewin, A. V. Kretinin, J. D. Caldwell, K. S. Novoselov, T. Taniguchi, K. Watanabe, F. Gaussmann, and T. Taubner, "Hyperbolic phonon-polaritons in boron nitride for near-field optical imaging and focusing," Nat. Commun. **6**, 7507 (2015).
[11]J. D. Caldwell, I. Aharonovich, G. Cassabois, J. H. Edgar, B. Gil, and D. Basov, "Photonics with hexagonal boron nitride," Nat. Rev. Mater. **4**, 552–567 (2019).
[12]Y. Kubota, K. Watanabe, O. Tsuda, and T. Taniguchi, "Deep ultraviolet light-emitting hexagonal boron nitride synthesized at atmospheric pressure," Science **317**, 932–934 (2007).
[13]G. Grosso, H. Moon, B. Lienhard, S. Ali, D. K. Efetov, M. M. Furchi, P. Jarillo-Herrero, M. J. Ford, I. Aharonovich, and D. Englund, "Tunable and high-purity room temperature single-photon emission from atomic defects in hexagonal boron nitride," Nat. Commun. **8**, 705 (2017).
[14]A. Joseph, V. Gautham, K. Akshay, and V. Sajith, "2D MoS_2-hBN hybrid coatings for enhanced corrosion resistance of solid lubricant coatings," Surf. Coat. Technol. **443**, 128612 (2022).
[15]A. Felicelli, I. Katsamba, F. Barrios, Y. Zhang, Z. Guo, J. Peoples, G. Chiu, and X. Ruan, "Thin layer lightweight and ultrawhite hexagonal boron nitride nanoporous paints for daytime radiative cooling," Cell Rep. Phys. Sci. **3**, 101058 (2022).
[16]Z. Zhang, S. Hu, J. Chen, and B. Li, "Hexagonal boron nitride: A promising substrate for graphene with high heat dissipation," Nanotechnology **28**, 225704 (2017).
[17]M. Raza, A. Westwood, C. Stirling, and R. Ahmad, "Effect of boron nitride addition on properties of vapour grown carbon nanofiber/rubbery epoxy composites for thermal interface applications," Composites Sci. Technol. **120**, 9–16 (2015).
[18]J. Han, G. Du, W. Gao, and H. Bai, "An anisotropically high thermal conductive boron nitride/epoxy composite based on nacre-mimetic 3D network," Adv. Funct. Mater. **29**, 1900412 (2019).
[19]M. G. Rasul, A. Kiziltas, B. Arfaei, and R. Shahbazian-Yassar, "2D boron nitride nanosheets for polymer composite materials," npj 2D Mater. Appl. **5**, 56 (2021).
[20]P.-Y. Liao, K. Khot, S. Alajlouni, M. Snure, J. Noh, M. Si, Z. Zhang, A. Shakouri, X. Ruan, and D. Y. Peide, "Alleviation of self-heating effect in top-gated ultrathin In_2O_3 FETs using a thermal adhesion layer," IEEE Trans. Electron Devices **70**, 113–120 (2023).

[21]R. Peierls, "Zur kinetischen theorie der wärmeleitung in kristallen," Ann. Phys. **395**, 1055–1101 (1929).
[22]A. Maradudin and A. Fein, "Scattering of neutrons by an anharmonic crystal," Phys. Rev. **128**, 2589 (1962).
[23]A. Debernardi, S. Baroni, and E. Molinari, "Anharmonic phonon lifetimes in semiconductors from density-functional perturbation theory," Phys. Rev. Lett. **75**, 1819 (1995).
[24]A. Debernardi, "Phonon linewidth in III-V semiconductors from density-functional perturbation theory," Phys. Rev. B **57**, 12847 (1998).
[25]D. A. Broido, M. Malorny, G. Birner, N. Mingo, and D. Stewart, "Intrinsic lattice thermal conductivity of semiconductors from first principles," Appl. Phys. Lett. **91**, 231922 (2007).
[26]K. Esfarjani, G. Chen, and H. T. Stokes, "Heat transport in silicon from first-principles calculations," Phys. Rev. B **84**, 085204 (2011).
[27]L. Lindsay, C. Hua, X. Ruan, and S. Lee, "Survey of *ab initio* phonon thermal transport," Mater. Today Phys. **7**, 106–120 (2018).
[28]A. J. McGaughey, A. Jain, H.-Y. Kim, and B. Fu, "Phonon properties and thermal conductivity from first principles, lattice dynamics, and the Boltzmann transport equation," J. Appl. Phys. **125**, 011101 (2019).
[29]T. Feng and X. Ruan, "Quantum mechanical prediction of four-phonon scattering rates and reduced thermal conductivity of solids," Phys. Rev. B **93**, 045202 (2016).
[30]T. Feng, L. Lindsay, and X. Ruan, "Four-phonon scattering significantly reduces intrinsic thermal conductivity of solids," Phys. Rev. B **96**, 161201 (2017).
[31]J. S. Kang, M. Li, H. Wu, H. Nguyen, and Y. Hu, "Experimental observation of high thermal conductivity in boron arsenide," Science **361**, 575–578 (2018).
[32]F. Tian, B. Song, X. Chen, N. K. Ravichandran, Y. Lv, K. Chen, S. Sullivan, J. Kim, Y. Zhou, T.-H. Liu *et al.*, "Unusual high thermal conductivity in boron arsenide bulk crystals," Science **361**, 582–585 (2018).
[33]S. Li, Q. Zheng, Y. Lv, X. Liu, X. Wang, P. Y. Huang, D. G. Cahill, and B. Lv, "High thermal conductivity in cubic boron arsenide crystals," Science **361**, 579–581 (2018).
[34]X. Yang, T. Feng, J. Li, and X. Ruan, "Stronger role of four-phonon scattering than three-phonon scattering in thermal conductivity of III-V semiconductors at room temperature," Phys. Rev. B **100**, 245203 (2019).
[35]A. Kundu, X. Yang, J. Ma, T. Feng, J. Carrete, X. Ruan, G. K. Madsen, and W. Li, "Ultrahigh thermal conductivity of θ-phase tantalum nitride," Phys. Rev. Lett. **126**, 115901 (2021).
[36]Y. Xia, V. I. Hegde, K. Pal, X. Hua, D. Gaines, S. Patel, J. He, M. Aykol, and C. Wolverton, "High-throughput study of lattice thermal conductivity in binary rocksalt and zinc blende compounds including higher-order anharmonicity," Phys. Rev. X **10**, 041029 (2020).
[37]D. Guo, Z. Xu, H. Zhang, C. Li, J. Sun, X. Luo, and Y. Ma, "Anharmonic phonon renormalization assisted acoustic branch scattering induces ultralow thermal conductivity and high thermoelectric performance of 2D SnSe," J. Alloys Compd. **932**, 167525 (2023).
[38]O. Hellman, I. Abrikosov, and S. Simak, "Lattice dynamics of anharmonic solids from first principles," Phys. Rev. B **84**, 180301 (2011).
[39]Y. Xia, "Revisiting lattice thermal transport in PbTe: The crucial role of quartic anharmonicity," Appl. Phys. Lett. **113**, 073901 (2018).
[40]N. K. Ravichandran and D. Broido, "Unified first-principles theory of thermal properties of insulators," Phys. Rev. B **98**, 085205 (2018).
[41]X. Gu, S. Li, and H. Bao, "Thermal conductivity of silicon at elevated temperature: Role of four-phonon scattering and electronic heat conduction," Int. J. Heat Mass Transfer **160**, 120165 (2020).
[42]A. Jain, "Multichannel thermal transport in crystalline Tl_3VSe_4," Phys. Rev. B **102**, 201201 (2020).
[43]Y. Xia, K. Pal, J. He, V. Ozoliņš, and C. Wolverton, "Particlelike phonon propagation dominates ultralow lattice thermal conductivity in crystalline Tl_3VSe_4," Phys. Rev. Lett. **124**, 065901 (2020).
[44]P. Jiang, X. Qian, R. Yang, and L. Lindsay, "Anisotropic thermal transport in bulk hexagonal boron nitride," Phys. Rev. Mater. **2**, 064005 (2018).
[45]J. Tang, G. Li, Q. Wang, J. Zheng, L. Cheng, and R. Guo, "Effect of four-phonon scattering on anisotropic thermal transport in bulk hexagonal boron nitride by machine learning interatomic potential," Int. J. Heat Mass Transfer **207**, 124011 (2023).
[46]G. Kresse and J. Hafner, "*Ab initio* molecular dynamics for liquid metals," Phys. Rev. B **47**, 558 (1993).
[47]W. Kohn and L. J. Sham, "Self-consistent equations including exchange and correlation effects," Phys. Rev. **140**, A1133 (1965).
[48]G. Kresse and J. Furthmüller, "Efficiency of ab-initio total energy calculations for metals and semiconductors using a plane-wave basis set," Comput. Mater. Sci. **6**, 15–50 (1996).
[49]J. Serrano, A. Bosak, R. Arenal, M. Krisch, K. Watanabe, T. Taniguchi, H. Kanda, A. Rubio, and L. Wirtz, "Vibrational properties of hexagonal boron nitride: Inelastic x-ray scattering and *ab initio* calculations," Phys. Rev. Lett. **98**, 095503 (2007).
[50]G. Kern, G. Kresse, and J. Hafner, "*Ab initio* calculation of the lattice dynamics and phase diagram of boron nitride," Phys. Rev. B **59**, 8551 (1999).
[51]C. Yuan, J. Li, L. Lindsay, D. Cherns, J. W. Pomeroy, S. Liu, J. H. Edgar, and M. Kuball, "Modulating the thermal conductivity in hexagonal boron nitride via controlled boron isotope concentration," Commun. Phys. **2**, 43 (2019).
[52]R. Cuscó, B. Gil, G. Cassabois, and L. Artús, "Temperature dependence of Raman-active phonons and anharmonic interactions in layered hexagonal BN," Phys. Rev. B **94**, 155435 (2016).
[53]S. Baroni, S. De Gironcoli, A. Dal Corso, and P. Giannozzi, "Phonons and related crystal properties from density-functional perturbation theory," Rev. Mod. Phys. **73**, 515 (2001).
[54]A. Togo and I. Tanaka, "First principles phonon calculations in materials science," Scr. Mater. **108**, 1–5 (2015).
[55]H. Zhou, S. Zhou, Z. Hua, K. Bawane, and T. Feng, "Extreme sensitivity of higher-order interatomic force constants and thermal conductivity to the energy surface roughness of exchange-correlation functionals," Appl. Phys. Lett. **123**, 192201 (2023).
[56]B. Niu, L. Zhong, W. Hao, Z. Yang, X. Duan, D. Cai, P. He, D. Jia, S. Li, and Y. Zhou, "First-principles study of the anisotropic thermal expansion and thermal transport properties in h-BN," Sci. China Mater. **64**, 953 (2021).
[57]W. Paszkowicz, J. Pelka, M. Knapp, T. Szyszko, and S. Podsiadlo, "Lattice parameters and anisotropic thermal expansion of hexagonal boron nitride in the 10–297.5 K temperature range," Appl. Phys. A **75**, 431–435 (2002).
[58]O. Hellman, P. Steneteg, I. A. Abrikosov, and S. I. Simak, "Temperature dependent effective potential method for accurate free energy calculations of solids," Phys. Rev. B **87**, 104111 (2013).
[59]O. Hellman and I. A. Abrikosov, "Temperature-dependent effective third-order interatomic force constants from first principles," Phys. Rev. B **88**, 144301 (2013).
[60]Z. Han, X. Yang, W. Li, T. Feng, and X. Ruan, "Fourphonon: An extension module to ShengBTE for computing four-phonon scattering rates and thermal conductivity," Comput. Phys. Commun. **270**, 108179 (2022).
[61]W. Li, J. Carrete, N. A. Katcho, and N. Mingo, "ShengBTE: A solver of the Boltzmann transport equation for phonons," Comput. Phys. Commun. **185**, 1747–1758 (2014).
[62]Y. Wei, X. You, H. Yang, Z. Luan, and D. Qian, "Towards GPU acceleration of phonon computation with ShengBTE," in *Proceedings of the International Conference on High Performance Computing in Asia-Pacific Region* (HPCAsia 2020) (Association for Computing Machinery, New York, NY, 2020), pp. 32–42.
[63]B. Zhang, Z. Fan, C. Zhao, and X. Gu, "GPU_PBTE: An efficient solver for three and four phonon scattering rates on graphics processing units," J. Phys. **33**, 495901 (2021).
[64]Z. Guo, P. R. Chowdhury, Z. Han, Y. Sun, D. Feng, G. Lin, and X. Ruan, "Fast and accurate machine learning prediction of phonon scattering rates and lattice thermal conductivity," Npj Comput. Mater. **9**, 95 (2023).
[65]Z. Guo, Z. Han, D. Feng, G. Lin, and X. Ruan, "Sampling-accelerated prediction of phonon scattering rates for converged thermal conductivity and radiative properties," npj Comput. Mater. **10**, 31 (2024).
[66]J. H. Warner, M. H. Rummeli, A. Bachmatiuk, and B. Buchner, "Atomic resolution imaging and topography of boron nitride sheets produced by chemical exfoliation," ACS Nano **4**, 1299–1304 (2010).

[67]H. J. Park, J. Cha, M. Choi, J. H. Kim, R. Y. Tay, E. H. T. Teo, N. Park, S. Hong, and Z. Lee, "One-dimensional hexagonal boron nitride conducting channel," Sci. Adv. **6**, eaay4958 (2020).
[68]G. Constantinescu, A. Kuc, and T. Heine, "Stacking in bulk and bilayer hexagonal boron nitride," Phys. Rev. Lett. **111**, 036104 (2013).
[69]E. Sichel, R. Miller, M. Abrahams, and C. Buiocchi, "Heat capacity and thermal conductivity of hexagonal pyrolytic boron nitride," Phys. Rev. B **13**, 4607 (1976).
[70]H. Salihoglu, V. Iyer, T. Taniguchi, K. Watanabe, P. D. Ye, and X. Xu, "Energy transport by radiation in hyperbolic material comparable to conduction," Adv. Funct. Mater. **30**, 1905830 (2020).
[71]G. Qin, Z. Qin, H. Wang, and M. Hu, "Anomalously temperature-dependent thermal conductivity of monolayer GaN with large deviations from the traditional $1/T$ law," Phys. Rev. B **95**, 195416 (2017).
[72]H. Wang, L. Yu, J. Xu, D. Wei, G. Qin, Y. Yao, and M. Hu, "Intrinsically low lattice thermal conductivity of monolayer hexagonal aluminum nitride (*h*-AlN) from first-principles: A comparative study with graphene," Int. J. Therm. Sci. **162**, 106772 (2021).
[73]H. Wang, G. Qin, G. Li, Q. Wang, and M. Hu, "Low thermal conductivity of monolayer ZnO and its anomalous temperature dependence," Phys. Chem. Chem. Phys. **19**, 12882–12889 (2017).